Optica Applicata, Vol. XLI, No. 3, 2011

Modeling of low-frequency modal noise induced by multimode couplers in cascade connections

ŁUKASZ MAKSYMIUK*, JERZY SIUZDAK

Institute of Telecommunications, Warsaw University of Technology,
Nowowiejska 15/19, 00-665, Warsaw, Poland

*Corresponding author: maksymiuk@tele.pw.edu.pl

In this paper, we present a theory concerning low-frequency modal noise in the cascade of couplers. This theory enables calculation of signal-to-noise ratio in cascade connection of multimode couplers. We provide a series of numerical calculations based on the model for different realizations of the couplers.

Keywords: modal noise, multimode fiber, multimode coupler, passive optical network (PON).

1. Introduction

In recent years, we have observed an increasing interest in the use of multimode fibers for short range connections [1]. A number of different multiplexation schemes [2, 3], excitation types [4] and topologies [5] of such networks have been proposed. One of the interesting approaches to the short range networks is a passive topology based on multimode fibers and couplers. Passive networks are widely used in access networks employing single mode fibers. However, the use of multimode fibers in PONs causes some problems, one of which is the variation of modal bandwidth in different branches of such networks, and the other is modal noise. Modal noise induced by some spatial light filtering induced by misaligned connectors was widely studied in the past years [6–9]. However, there are only a few papers considering modal noise induced by multimode couplers [10, 11] and no papers considering theoretical analysis of modal noise induced by couplers connected in a cascade or generally in more complex connections (as is common in a variety of PONs topologies). This article is meant to fill in this gap. We provide a theory which describes modal noise in more complex configuration of couplers configurations (as a cascade of couplers), moreover we show a series of numerical simulations based on the model. These simulations may be confronted with a series of measurements that we have published in [12].

2. Theory

The principle of modal noise emerging in couplers/splitter is as follows: firstly, modes coupling from the input port to the different output ports are slightly different, *i.e.*, the power distribution among the modes in output ports is generally different; secondly, this distribution in output ports depends on phase dependencies at the input port; thirdly, phase dependencies at the input vary due to vibrations and changes of temperature. Varying distribution in modes at a particular output port also means a change of total power at this port, namely the total power at all output ports of the coupler is more or less constant, but the division among the ports changes (as shown in Fig. 1). Therefore at a particular output port one observes fluctuation of power, which may be treated as modal noise induced by the coupler.

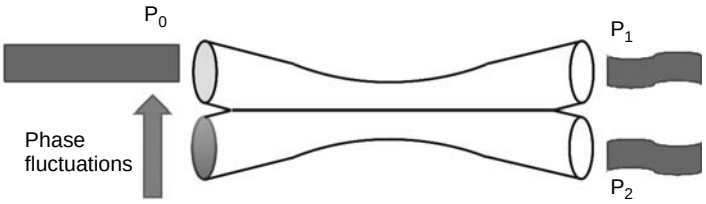

Fig. 1. Varying total power distribution between coupler arms; the powers in coupler arms slightly vary whereas their sum $P_0 = P_1 + P_2$ is constant.

The theory presented in this section is consistent with that presented in [8]. However, in that paper it was used to describe modal noise induced by misaligned connectors, whereas we adopted it to describe modal noise induced by couplers. Incident field at the input of the coupler is given by:

$$A_{\text{in}}(x, y) = \sum_i a_i \varphi_i(x, y) \tag{1}$$

where $\varphi_i(x, y)$ is two-dimensional field distribution and a_i is its complex representation given by:

$$a_i = |a_i| \exp\left\{ j\left[2\pi f_0(t - \tau_i) + \varphi(t - \tau_i) + \theta_i(t) \right] \right\} \tag{2}$$

In the equation above: f_0 is the optical frequency, φ represents phase noise of the light source, τ_i is a temporal delay along the path between light source and coupler, and θ_i is the phase shift along the same path. By exciting coupler with the i-th mode, we obtain the resultant field at the output of the coupler given by:

$$A^i_{\text{out}}(x, y) = \sum_i b_{ij} \psi_i(x, y) \tag{3}$$

where: ψ_i is a spatial distribution of the output mode field and b_{ij} is a complex coupling coefficient that is expressed as:

$$b_{ij} = |b_{ij}| \exp(j\varphi_{ij}) \tag{4}$$

The coupler is linear, therefore assuming that excitation is given by (1), the output filed at a particular output port may be expressed by:

$$A_{\text{out}}(x, y) = \sum_i \sum_j a_i b_{ij} \psi_i(x, y) \tag{5}$$

The output power at the particular output port of the coupler at a given time moment is expressed by:

$$\begin{aligned} P_{\text{out}}(t) &= \iint_A A_{\text{out}}(x, y) A^*_{\text{out}}(x, y) \mathrm{d}x\mathrm{d}y = \\ &= \sum_i \sum_j \sum_k \sum_m a_i b_{ij} a^*_k b^*_{km} \iint_A \psi_j(x, y)\, \psi^*_m(x, y) \mathrm{d}x\mathrm{d}y = \\ &= \sum_i \sum_k \sum_j a_i b_{ij} a^*_k b^*_{kj} = \sum_i \sum_k a_i\, a^*_k F_{ik} \end{aligned} \tag{6}$$

In the above equation, F_{ik} is a complex coupling coefficient describing the amount of power transferred from the input mode i to the output mode k. In general, these coefficients may also describe some other mode filtering device such as a misaligned connector. However, in the case of a connector F_{ik} there are real values, whereas for the coupler these coefficients are complex in general. Substituting (2) into (6) and assuming that $P_i = |a_i|^2$ we may transform (6) into:

$$P_{\text{out}}(t) = \sum_i \sum_k \sqrt{P_i P_k}\, |F_{ik}| \exp\left\{ j\left[-2\pi f_0 \tau_{ik} + \varphi(t - \tau_i) - \varphi(t - \tau_k) + \Theta_{ik}(t) + \Delta_{ik} \right] \right\} \tag{7}$$

The average value of the output power is:

$$\begin{aligned} E\left[P_{\text{out}}\right] &= \sum_i \sum_k \sqrt{P_i P_k}\, |F_{ik}| \cdot \\ &\quad \cdot E\left[\exp\left\{ j\left[-2\pi f_0 \tau_{ik} + \varphi(t - \tau_i) - \varphi(t - \tau_k) + \Theta_{ik}(t) + \Delta_{ik} \right] \right\} \right] = \\ &= \sum_i P_i F_{ii} \end{aligned} \tag{8}$$

where P_i is a power of the i-th input mode and is given by:

$$P_i = |a_i|^2 \tag{9}$$

The last form of Equation (8) is so simple because for every $i \neq k$ variable Θ_{ik} is a random value, therefore its expected value is zero. Now, let us write the relationship for covariance:

$$\begin{aligned}
\mathrm{cov}_{P_{\mathrm{out}}}(\Delta t) &= E\left[P_{\mathrm{out}}(t)\, P^*_{\mathrm{out}}(t+\Delta t)\right] - \left\{E\left[P_{\mathrm{out}}\right]\right\}^2 = \\
&= E\left\{\left[P_{\mathrm{out}}(t) - E\left(P_{\mathrm{out}}(t)\right)\right]\left[P^*_{\mathrm{out}}(t+\Delta t) - E\left(P^*_{\mathrm{out}}(t)\right)\right]\right\} = \\
&= \sum_i \sum_k \sum_m \sum_n \sqrt{P_i P_k P_m P_{ni}}\, |F_{ik}||F_{mn}| \cdot \\
&\cdot E\Big(j\big[-2\pi f_0 \tau_{ik} + 2\pi f_0 \tau_{mn} + \Delta_{ik} - \Delta_{mn} + \Theta_{ik}(t) - \Theta_{mn}(t+\Delta t) + \\
&+ \varphi(t-\tau_i) - \varphi(t-\tau_k) - \varphi(t+\Delta t-\tau_m) + \varphi(t+\Delta t-\tau_n)\big]\Big)
\end{aligned} \tag{10}$$

Similarly as in Equation (7), variable Θ_{ik} is random value for every $i \neq k$, therefore expected value of the exponent function in (10) is non-zero only in two cases:

1) $i = k$ and $m = n$,
2) $i = m$ and $k = n$.

Taking this assumption we may transform (10) into:

$$\begin{aligned}
\mathrm{cov}_{P_{\mathrm{out}}}(\Delta t) &= \sum_i \sum_k P_i P_k F_{ii} F_{kk} + \sum_i \sum_{\substack{k \\ k \neq i}} P_i P_k |F_{ik}|^2 \cdot \\
&\cdot E\left(\exp\left\{j\left[\Theta_{ik}(t) - \Theta_{ik}(t+\Delta t) + \varphi(t-\tau_i) - \varphi(t-\tau_k) + \right.\right.\right. \\
&\left.\left.\left. - \varphi(t+\Delta t-\tau_i) + \varphi(t+\Delta t-\tau_k)\right]\right\}\right) - \left(\sum_i P_i F_{ii}\right)^2 = \\
&= \sum_i \sum_{\substack{k \\ k \neq i}} P_i P_k |F_{ik}|^2 E\left(\exp\left\{j\left[\Theta_{ik}(t) - \Theta_{ik}(t+\Delta t) + \right.\right.\right. \\
&\left.\left.\left. + \varphi(t-\tau_i) - \varphi(t-\tau_k) - \varphi(t+\Delta t-\tau_i) + \varphi(t+\Delta t-\tau_k)\right]\right\}\right)
\end{aligned} \tag{11}$$

Assuming that fluctuations of the mode phases in the fiber (induced by ambient factors, such as temperature variations or stress inducing vibrations) are independent of phase noise of the light source, we may express covariance of the output power as:

$$\operatorname{cov}_{P_{\text{out}}}(\Delta t) = \sum_i \sum_{\substack{k \\ k \neq i}} P_i P_k |F_{ik}|^2 E\left[\exp\left\{j\left(\Theta_{ik}(t) - \Theta_{ik}(t+\Delta t)\right)\right\}\right] \cdot$$
$$\cdot E\left[\exp\left\{j\left(\varphi(t-\tau_i) - \varphi(t-\tau_k) - \varphi(t+\Delta t-\tau_i) + \varphi(t+\Delta t-\tau_k)\right)\right\}\right] \tag{12}$$

Let us assume that the phase noise of the light source is Gaussian and that variance of phase changes during the time τ of the measurement is given by [13]:

$$E\left[(\Delta\varphi)^2\right] = E\left\{\left[\varphi(t+\tau) - \varphi(t)\right]^2\right\} = 2\pi B_{\text{FWHM}}\,\tau \tag{13}$$

By making assumptions as stated above, we conclude the light source to be Lorentzian and B_{FWHM} is a full width of the spectrum measured at half maximum. Similar assumptions are also made for phase changes (denoted as Θ) and signal spectrum in fiber. By taking the well known relationship for Gaussian variables having zero mean value ($E[e^{jx}] = e^{-0.5E(x^2)}$) and taking into account the fact that phase changes in separate periods are independent, we may transform (12) into:

$$\operatorname{cov}_{P_{\text{out}}}(\Delta t) = \sum_i \sum_{\substack{k \\ k \neq i}} P_i P_k |F_{ik}|^2 \exp\left(-\pi B_L |\Delta t|\right) \exp\left\{-2\pi B_{\text{FWHM}}\, g(|\Delta t|)\right\} \tag{14}$$

where:

$$g(\Delta t) = \begin{cases} |\Delta t|, & |\Delta t| \leq |\tau_{ik}| \\ |\tau_{ik}|, & |\Delta t| > |\tau_{ik}| \end{cases} \tag{15}$$

In Equation (14), B_L is the bandwidth of the low frequency modal noise, which is typically less than some hundreds of Hz [14]. For the typical light sources used in telecommunications $B_L \ll B_{\text{FWHM}}$, therefore we may transform Eq. (14) into:

$$\operatorname{cov}_{P_{\text{out}}}(\Delta t) = \exp\left\{-\pi B_L |\Delta t|\right\} \sum_i \sum_{\substack{k \\ k \neq i}} P_i P_k |F_{ik}|^2 \cdot$$

$$\cdot \left\{ \mathrm{Sa}\left(\frac{\Delta t}{\tau_{ik}} \right) \left[\exp\left(-2\pi B_{\mathrm{FWHM}} |\Delta t| \right) - \exp\left(-2\pi B_{\mathrm{FWHM}} |\tau_{ik}| \right) \right] + \right.$$

$$\left. + \exp\left(-2\pi B_{\mathrm{FWHM}} |\tau_{ik}| \right) \right\} \approx$$

$$\approx \exp\left(-\pi B_L |\Delta t| \right) \sum_i \sum_{\substack{k \\ k \neq i}} P_i P_k |F_{ik}|^2 \exp\left(-2\pi B_{\mathrm{FWHM}} |\tau_{ik}| \right) +$$

$$+ \sum_i \sum_{\substack{k \\ k \neq i}} P_i P_k |F_{ik}|^2 \, \mathrm{Sa}\left(\frac{\Delta t}{\tau_{ik}} \right) \cdot$$

$$\cdot \left[\exp\left(-2\pi B_{\mathrm{FWHM}} |\Delta t| \right) - \exp\left(-2\pi B_{\mathrm{FWHM}} |\tau_{ik}| \right) \right] \tag{16}$$

where:

$$\mathrm{Sa}(x) = \begin{cases} 1, & |x| \leq 1 \\ 0, & |x| > 1 \end{cases} \tag{17}$$

In Equation (16) there are two terms. The first one is a low frequency noise (its bandwidth is B_L) caused by phase fluctuations Θ of particular modes. The second one is a high frequency noise which is caused by non-monochromatic nature of the light source and modulation of the linewidth of the light source or by mode partition noise in multimode lasers [15]. The topic of this paper is the low frequency modal noise, therefore in further divagations we will neglect the high frequency modal noise.

Having covariance given by (16) we can express the variance for the low frequency modal noise as:

$$\mathrm{var}_{P_{\mathrm{out}}} = \sum_i \sum_{\substack{k \\ k \neq i}} P_i P_k |F_{ik}|^2 \exp\left\{ -2\pi B_{\mathrm{FWHM}} |\tau_{ik}| \right\} \tag{18}$$

By taking into account equations (18) and (8) we obtain the equation for the electrical signal-to-noise ratio in the presence of the low frequency modal noise induced by the coupler:

$$\mathrm{SNR}_e = \frac{\left(\sum_i P_i F_{ij} \right)^2}{\sum_i \sum_{\substack{k \\ k \neq i}} P_i P_k |F_{ik}|^2 \exp\left\{ -2\pi B_{\mathrm{FWHM}} |\tau_{ik}| \right\}} \tag{19}$$

In general, F_{ik} may be expressed as

$$F_{ik} = \sum_j |b_{ij}||b_{kj}| \exp\left[j(\varphi_{ij} - \varphi_{kj}) \right] = \sum_j b_{ij}\, b_{kj}^* \tag{20}$$

where b_{ij} and b_{kj} are complex amplitude coupling coefficients. For F_{ii} elements, the equation above reduces to:

$$F_{ii} = \sum_j |b_{ij}||b_{ij}| \exp\left[j(\varphi_{ij} - \varphi_{ij}) \right] = \sum_j |b_{ij}|^2 \tag{21}$$

In Equation (19), the term $\exp\{-2\pi B_{\mathrm{FWHM}}|\tau_{ik}|\}$ is called the speckle pattern contrast [7], and it changes along the fiber. At the front end of the fiber $B_{\mathrm{FWHM}}\tau_{ik} \ll 1$ and term $\exp\{-2\pi B_{\mathrm{FWHM}}|\tau_{ik}|\}$ is almost equal to 1 (this is the full coherence case), then it decreases (the partial coherence case). When $\exp\{-2\pi B_{\mathrm{FWHM}}|\tau_{ik}|\} \to 0$ the modal noise vanishes (it is the non-coherence case).

3. Numerical simulations

Based on the theory presented in the previous section we performed a series of numerical simulations to calculate electrical SNR versus the number of couplers in the cascade connection. First of all we needed to calculate b_{ij} (see Eq. (20)), *i.e.*, complex amplitude coupling coefficients describing the amount of power being transferred from a particular mode at the input to particular modes at the output ports. We used similar methods as those described in [5]. We solved simplified wave equation [16]:

$$\left\{ j2\pi n_2 \frac{\partial}{\partial z} + \frac{\partial^2}{\partial x^2} + \frac{\partial^2}{\partial y^2} + k^2 \left[n_1^2(x, y, z) - n_2^2 \right] \right\} E(x, y, z) = 0 \tag{22}$$

numerically for every input mode i. In Equation (22), n_2 stands for a refraction coefficient of cladding, $n(x, y, z)$ represents a refraction profile of the core (that changes with z and depends on the particular geometry of the coupler), k is the wave number and $E(x, y, z)$ is a complex amplitude of the electrical field.

Every solution gave complex resultant fields for two output ports. In the next step, we decomposed these fields into orthogonal set of modes by calculating appropriate integrals numerically:

$$b_{ij} = \iint_S \mathrm{d}x\mathrm{d}y\, \varphi_j^*(x, y) E_i(x, y, z = \mathrm{end}) \tag{23}$$

In the equation above, $E_i(x, y, z = \mathrm{end})$ is the resultant field at the end of a particular output port of the coupler and $\varphi_j^*(x, y)$ is the field of the j-th LP mode. This decomposition led us to b_{ij} coupling coefficients. We calculated a set of b_{ij} coefficients

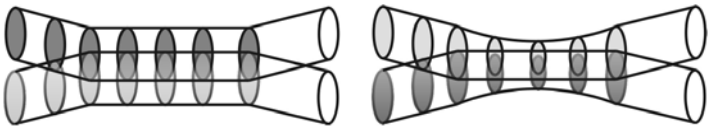

Fig. 2. Coupler structures analyzed; on the left polished coupler, on the right biconical taper coupler structure (fiber radii are significantly decreased in the inner part of the coupler).

for different realizations of biconical fused taper coupler structures and non-tapered symmetrical polished coupler (see Fig. 2). Matrix B_{ij} of b_{ij} coefficients, let us call it couplers' transfer matrix, represents a particular coupler. The resultant matrix of the cascade interconnection of two different couplers *a* and *b* represented respectively by matrices $B_{ij}^{(a)}$ and $B_{ij}^{(b)}$ may be simply obtained as a multiplication of these matrices. A similar operation may be performed for more than two couplers.

With the use of the calculated coupling coefficients for the different realizations of couplers (and configurations, *i.e.*, interconnections in the cascade) and with the use of Eq. (20) we performed calculation of electrical SNR versus the number of couplers in the cascade.

In the first example, we assumed the coupler to be biconical fused taper. For this coupler, we have analyzed two cases: a fully coherent light case (results in Fig. 3) and light with partial coherence (results in Fig. 4). In the partial coherence spectral linewidth was assumed to be $\Delta\lambda = 0.2$ nm and length $l = 50$ m (as it was in the measurements provided in [12]).

In the second example (Fig. 5), we took into account a polished coupler. As previously spectral linewidth was assumed to be $\Delta\lambda = 0.2$ nm and length $l = 50$ m. The reason for that was to show a significant influence of coupler's geometry on the amount of modal noise.

In Figures 3, 4 and 5, we clearly see an SNR decrease with the increasing number of couplers. However, for the totally coherent light (Fig. 3) values of SNR are significantly lower than for the partially coherent case. Moreover, there is a significant difference between biconical fused taper couplers and polished ones. The latter has

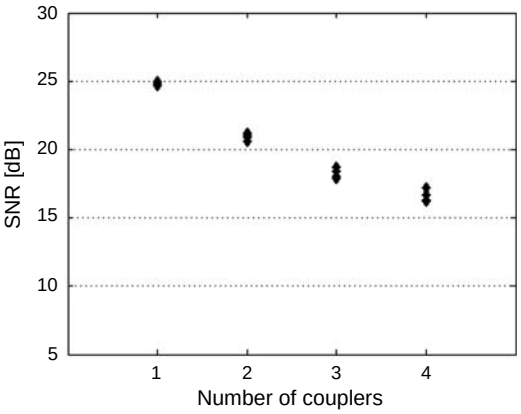

Fig. 3. SNR versus number of couplers in the cascade; coherent light – biconical taper couplers.

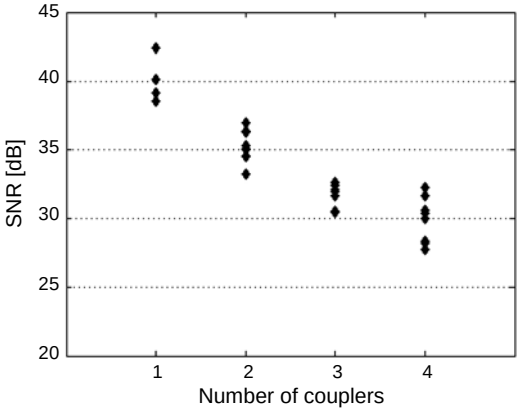

Fig. 4. SNR versus number of couplers in the cascade; partially coherent light – biconical taper couplers.

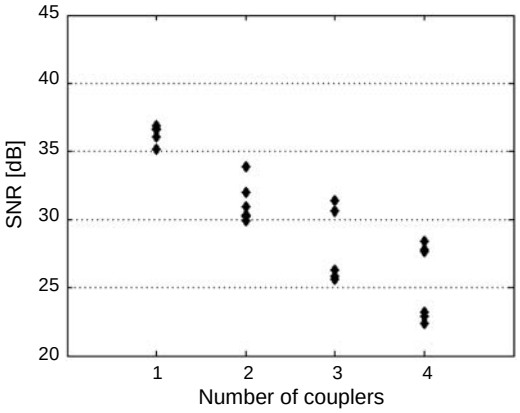

Fig. 5. SNR versus number of couplers in the cascade; partially coherent light – polished couplers.

significantly lower SNR. The reason is that the tapered couplers exhibit more uniform mode power distribution in two output ports than polished couplers. In polished couplers there is a strong tendency of the lower order modes being more pronounced in the excited arm of the coupler, whereas the higher order modes are coupled to the other arm. The conclusion is that the more uniform the power distribution in output ports of the coupler, the lower the modal noise is, regardless the coupler exact design (geometry).

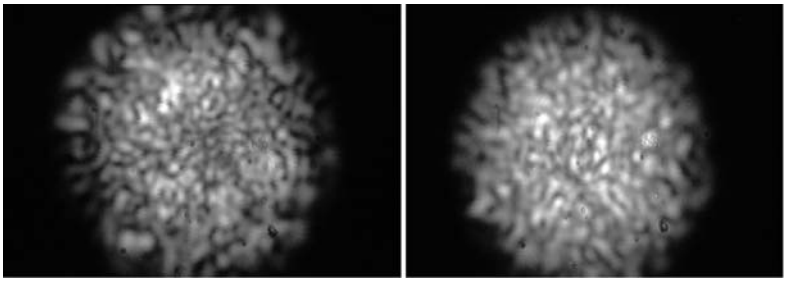

Fig. 6. CCD camera snapshots of far field distributions in two output ports of the coupler.

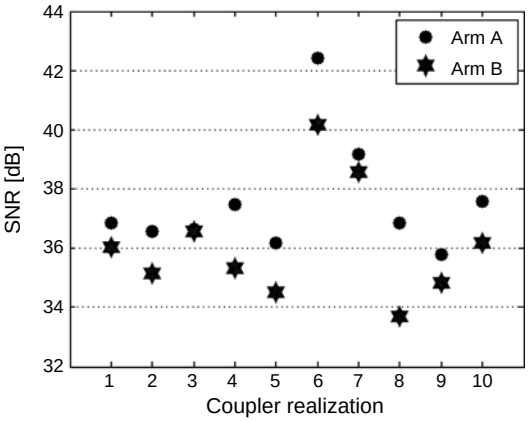

Fig. 7. SNR in two couplers' arms; different realizations of couplers structures; partially coherent light.

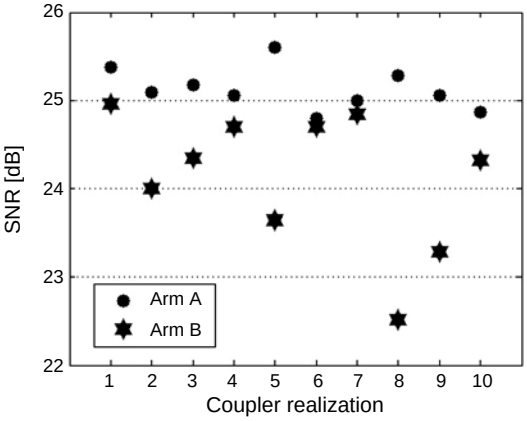

Fig. 8. SNR in two couplers' arms; different realizations of couplers structures; fully coherent light.

As was mentioned above the distribution of modes at different output ports of the coupler is different, in general. The fact is visible in Fig. 6, where far field patterns obtained by CCD camera at the output ports of polished coupler are shown. This indicates that these two output ports may exhibit different modal noise. Let us now take a closer look at these differences for two output ports. The results are shown in Figs. 7 and 8, for partial coherent case (assumed parameters: $\Delta\lambda = 0.2$ nm, $l = 50$ m) and coherent case, respectively. The images presented show SNR results for different realizations of couplers in both arms. Arm denoted as A is the excited one, whereas B is the arm to which the optical power is coupled. It is clearly visible that arm A has a tendency to exhibit better SNR in general for all realizations of the couplers. Similarly as before fully coherent case gave worse results than partial coherent one. However, it is worth mentioning that a coupler of a particular structure may exhibit high deviation of SNR between arms for a particular degree of coherence of light and low deviation

of SNR for other degree of coherence. For example, coupler denoted as 6 has high deviation of SNR for partial coherence case (Fig. 7) and low for total coherence (Fig. 8); on the other hand, coupler number 8 behaves reversely.

4. Conclusions

In this paper, we have presented theory and numerical simulations concerning modal noise induced by the cascade of multimode couplers/splitters. We have considered theoretically two cases: the fully coherent light and the partially coherent light. The fully coherent light is the worst scenario producing lowest SNRs (which is clearly visible when we compare Figs. 3 and 4). However, when we consider differences in the SNR reduction with the increasing number of couplers, it is similar for both cases (coherent and partially coherent). In paper [12], we provided a series of measurements; when we compare them with the numerical results (the partially coherent case) we notice a similar behavior, *i.e.*, a significant decrease of SNR versus an increasing number of couplers. However, the measurements show a more rapid decrease of SNR than the numerical results. These discrepancies of the measurements and the numerical simulations may be caused by two factors: the design (its geometrical structure) of the coupler used in the experiment was unknown (it is also impossible to obtain geometrical structure of the coupler with the use of some measurements) and we did know the exact linewidth of the light source. Concluding, we have shown, both numerically and theoretically, that modal noise in the cascade of multimode couplers is an important issue and may cause significant degradation of SNR. It is very important when one may consider PON based on multimode fibers and couplers. Namely, it will reduce the possible number of couplers in the cascade. We have also developed a theory that may be used for numerical modeling of modal noise in the passive structures based on multimode components.

Acknowledgements – This work has been supported (for L. Maksymiuk) by the European Union in the framework of European Social Fund through the Warsaw University of Technology Development Programme, realized by Center for Advanced Studies.

References

[1] Freund R.E., Bunge C.-A., Ledentsov N.N., Molin D., Caspar C., *High-speed transmission in multimode fibers*, IEEE Journal of Lightwave Technology **28**(4), 2010, pp. 569–586.

[2] Tsekrekos C.P., De Boer M., Martinez A., Willems F.M.J., Koonen A.M.J., *Demonstration of a transparent 2-input 2 output mode group diversity multiplexing link*, Proceedings of the European Conference on Optical Communications, ECOC'06, 2006, paper no. We3.P.145.

[3] Raddatz L., White I.H., *Overcoming the modal bandwidth limitation of multimode fiber by using passband modulation*, IEEE Photonics Technology Letters **11**(2), 1999, pp. 266–268.

[4] Raddatz L., White I.H., Cunningham D.G., Nowell M.C., *An experimental, theoretical study of the offset launch technique for the enhancement of the bandwidth of multimode fiber links*, IEEE Journal of Lightwave Technology **16**(3), 1998, pp. 324–331.

[5] STĘPNIAK G., MAKSYMIUK Ł., SIUZDAK J., *A numerical model of multimode fiber PON frequency response*, Optical and Quantum Electronics **39**(15), 2007, pp. 1281–1288.
[6] RAWSON E.G., GOODMAN J.W., NORTON R.E., *Frequency dependance of modal noise in multimode optical fibers*, Jurnal of Optical Society of America **70**(8), 1980, pp. 968–976.
[7] PEPELJUGOSKI P., KUCHTA D., RISTESKI A., *Modal noise BER calculations in 10 Gbit/s multimode fiber LAN links*, IEEE Photonics Technology Letters **17**(12), 2005, pp. 2586–2588.
[8] PETERMANN K., *Nonlinear distortions and noise in optical communications systems due to fiber connectors*, IEEE Journal of Quantum Electronics **16**(7), 1980, pp. 761–770.
[9] WEGMULLER M., GOLOWICH S., GIARETTA G., NUSS M., *Evolution for the beam diameter in a multimode fiber link through offset connectors*, IEEE Photonics Technology Letters **14**(6), 2001, pp. 574–576.
[10] KAWASAKI B.S., HILL K.O., TREMBLAY Y., *Modal noise generation in biconical-taper coupler*, Optics Letters **6**(10), 1980, pp. 499–501.
[11] SEVERIN P.J., BARDOEL W.H., *Bandwidth and modal noise effects in fused-head-end multimode fiber passive components*, IEEE Journal of Lightwave Technology **7**(12), 1989, pp. 1932–1940.
[12] SIUZDAK J., SADKOWSKA A., MAKSYMIUK Ł., STĘPNIAK G., *Modal noise in cascaded multimode splitters*, Asia Optical Fiber Communication and Optoelectronic Exposition and Conference AOE, 2008, pp. 17–23.
[13] GARRETT I., JACOBSEN G., *Theoretical analysis of heterodyne optical receivers for transmission systems using (semiconductor) lasers with nonnegligible linewidth*, IEEE Journal of Lightwave Technology **4**(3), 1986, pp. 323–334.
[14] SHIHONARA H., *Modal-noise characteristics in aerial optical cables subjected to vibration*, IEEE Journal of Lightwave Technology **1**(4), 1983, pp. 535–541.
[15] DANDLIKER R., BERTHOLDS A., MAYSTRE F., *How modal noise in multimode fiber depends on source spectrum and fiber dispersion*, IEEE Journal of Lightwave Technology **3**(1), 1985, pp. 7–12.
[16] YEH C., BROWN W.P., SZEJN R., *Multimode inhomogeneus fiber couplers*, Applied Optics **18**(4), 1978, pp. 489–495.

Received November 19, 2010